

# NNLO corrections to inclusive semileptonic $B$ decays in the shape-function region

Guido Bell

*Institut für Theoretische Teilchenphysik, Universität Karlsruhe, D-76128 Karlsruhe, Germany*

Received 6 November 2008; accepted 17 December 2008

Available online 25 December 2008

---

## Abstract

We compute 2-loop QCD corrections to the hard coefficient functions which arise in the factorization formula for  $B \rightarrow X_u \ell \nu$  decays in the shape-function region. Our calculation provides the last missing piece required for a NNLO analysis of inclusive semileptonic  $B$  decays, which may significantly reduce the theoretical uncertainty in the extraction of the CKM matrix element  $|V_{ub}|$ . Among the technical aspects, we find that the 2-loop hard coefficient functions are free of infrared singularities as predicted by the factorization framework. We perform a brief numerical analysis of the NNLO corrections and include a discussion on charm mass effects.

© 2009 Elsevier B.V. All rights reserved.

---

## 1. Introduction

Charmless semileptonic  $B$  meson decays are mediated by a  $b \rightarrow u$  quark transition. The study of inclusive and exclusive semileptonic  $B$  decays provide two independent paths for a determination of the strength of the flavour-changing interaction. In the Standard Model the quark transition is governed by the CKM matrix element  $V_{ub}$ , which constitutes an important input parameter for many analyses in flavour physics.

Since the determination of CKM matrix elements from exclusive semileptonic  $B$  meson decays requires the knowledge of non-perturbative form factors, the determination from inclusive semileptonic decays is a priori cleaner from the theoretical point of view. The total decay rate can be described by a local Operator Product Expansion (OPE) in a simultaneous expansion in  $\Lambda_{\text{QCD}}/m_b$  and  $\alpha_s(m_b)$  [1]. The local OPE can be applied for inclusive  $B \rightarrow X_c \ell \nu$  decays, where

---

*E-mail address:* [bell@particle.uni-karlsruhe.de](mailto:bell@particle.uni-karlsruhe.de).

the non-perturbative information is constrained to some numbers, HQET parameters, which can be extracted simultaneously with  $|V_{cb}|$  from an analysis of the  $B$  meson decay spectra.

A major complication arises in charmless semileptonic  $B$  decays where experimental measurements of the  $B \rightarrow X_u \ell \nu$  decay rate have to introduce kinematical cuts to suppress the  $B \rightarrow X_c \ell \nu$  background. This restricts the experimentally accessible information to the shape-function region in which the hadronic final state has large energy  $E_X \sim m_b$  but moderate invariant mass  $p_X^2 \sim m_b \Lambda_{\text{QCD}}$ . The theoretical description of partial decay rates in the shape-function region is more complicated and gives rise to a multi-scale OPE in terms of non-local light-cone operators.

The development of QCD Factorization [2] and Soft-Collinear Effective Theory (SCET) [3] has widely improved our understanding of strong interaction effects in charmless  $B$  meson decays. A factorization theorem for the partial  $B \rightarrow X_u \ell \nu$  decay rate in the shape-function region has originally been proposed in the diagrammatic approach [4] and has later been formulated in the operator formalism within SCET. The factorization formula can be expressed in terms of the hadronic tensor  $W^{\mu\nu}$ , which encodes the strong interaction effects in  $B \rightarrow X_u \ell \nu$  decays, schematically as

$$W^{\mu\nu} \sim \sum_{i,j} c_{ij}^{\mu\nu} H_{ij}(n+p) \int d\omega J(p_\omega^2) S(\omega), \quad (1)$$

with hard coefficient functions  $H_{ij}$ , a jet function  $J$  and a shape function  $S$  which describes the distribution of the residual light-cone momentum of the  $b$ -quark within the  $B$  meson [5] (the  $c$ 's are some tensor coefficients). Whereas the hard functions and the jet function can be computed in perturbation theory, since they describe fluctuations with virtualities  $\sim m_b^2$  and  $\sim \Lambda_{\text{QCD}} m_b$  respectively, the shape function represents a non-perturbative input to the factorization formula.

In this work we address perturbative corrections to the factorization formula (1). Next-to-leading order (NLO) corrections to the hard functions  $H_{ij}$  and the jet function  $J$  have been computed in [6] and next-to-next-to-leading order (NNLO) corrections to the jet function have been worked out in [7]. The only missing piece for a NNLO analysis of inclusive semileptonic  $B$  decays in the shape-function region consists in the  $\alpha_s^2$  corrections to the hard functions which we consider in this work.

A first step towards the computation of NNLO corrections to the hard functions has been taken recently in [8]. The authors of [8] computed 2-loop QCD corrections to the form factors which parameterize the  $b \rightarrow u$  quark transition. We present an independent calculation of these 2-loop form factors and extend the analysis of [8] in two respects: First, we perform the subsequent matching calculation within SCET to extract the hard functions  $H_{ij}$  from the form factors which are formally infrared divergent. Second, we keep a non-vanishing charm quark mass in our 2-loop calculation which has been set to zero in [8].

The 2-loop calculation that we present in this work is closely related to the calculation of NNLO vertex corrections in hadronic  $B$  decays which we considered in [9]. It is in fact somewhat simpler than the one in [9] since it involves only a small subset of Feynman diagrams and 2-loop integrals. A further complication arises in the analysis of [9] through the appearance of evanescent four-quark operators which makes the matching calculation rather involved.

The outline of this paper is as follows: To set up our notation, we briefly recapitulate the necessary ingredients for the matching calculation in Section 2. The 2-loop calculation of the QCD form factors is described in Section 3. We perform the matching calculation in Section 4, where we present our results for the NNLO hard coefficient functions  $H_{ij}$ . We extend our analysis to include charm mass effects in Section 5. We briefly analyze the numerical impact of the

NNLO corrections in Section 6, before we conclude in Section 7. We collect some results for the NLO and NNLO coefficient functions and for the charm mass dependent Master Integrals in Appendices A–C.

## 2. Preliminaries

The basic quantity for the analysis of strong interaction effects to inclusive semileptonic  $B$  meson decays is the hadronic tensor  $W^{\mu\nu}$ , which is defined via the discontinuity of the forward matrix element of the correlation function of two weak interaction currents  $J^\mu = \bar{u}\gamma^\mu(1 - \gamma_5)b$ ,

$$W^{\mu\nu} = \frac{1}{\pi} \text{Im} \langle B(p_B) | i \int d^4x e^{iqx} T [J^{\dagger\mu}(0) J^\nu(x)] | B(p_B) \rangle. \quad (2)$$

For the present analysis of inclusive semileptonic decays in the shape-function region it will be convenient to introduce light-cone coordinates. We introduce two light-like vectors  $n_\pm$  with  $n_\pm^2 = 0$  and  $n_+n_- = 2$ . Any four-vector can be decomposed according to its projections onto these light-cone directions and a two-dimensional transverse plane as

$$p^\mu = (n_+p) \frac{n_-^\mu}{2} + p_\perp^\mu + (n_-p) \frac{n_+^\mu}{2} \equiv (n_+p, p_\perp, n_-p). \quad (3)$$

In the shape-function region the momentum of the hadronic final state  $X_u$  scales as a hard-collinear momentum, i.e.  $p_X \sim m_b(1, \lambda, \lambda^2)$  with  $\lambda^2 = \Lambda_{\text{QCD}}/m_b$ . A factorization theorem for the hadronic tensor  $W^{\mu\nu}$  can be established in a two-step matching procedure  $\text{QCD} \rightarrow \text{SCET} \rightarrow \text{HQET}$ . In the first step hard fluctuations with virtuality  $\sim m_b^2$  are integrated out. The semileptonic current becomes to leading power in  $\lambda$

$$J^\mu(x) \simeq e^{-im_b v \cdot x} \sum_{i=1}^3 \int ds \tilde{C}_i(s) [\bar{\xi} W_{hc}] (x + sn_+) \Gamma_i^\mu h_v(x_-), \quad (4)$$

with the  $B$  meson velocity  $v$  and  $x_- = (n_+x)n_-/2$ . The static  $b$ -quark field  $h_v$  is defined in HQET and the hard-collinear  $u$ -quark field  $\xi$  and the Wilson line  $W_{hc}$  in SCET. The momentum space Wilson coefficients can be obtained via

$$C_i(n_+p) = \int ds e^{isn_+p} \tilde{C}_i(s). \quad (5)$$

In the second matching step hard-collinear fluctuations with virtuality  $\sim \Lambda_{\text{QCD}}m_b$  are integrated out. This gives rise to another perturbative coefficient function, the jet function  $J$ , and a remnant HQET matrix element, the shape function  $S$ . The factorization formula for the hadronic tensor becomes to leading power in  $\lambda$

$$W^{\mu\nu} \simeq \sum_{i,j=1}^3 H_{ij}(n_+p) \text{Tr} \left( \bar{\Gamma}_j^\mu \frac{\not{p}}{2} \Gamma_i^\nu \frac{1+\not{p}}{2} \right) \int d\omega J(p_\omega^2) S(\omega). \quad (6)$$

The hard functions  $H_{ij}$ , which we consider in this work, are related to the Wilson coefficients  $C_i$  of the semileptonic current by  $H_{ij} = C_i C_j$ . We may therefore mainly focus on the matching relation (4) instead of the factorization formula for the hadronic tensor (6).

The matching calculation simplifies if we work with on-shell quarks and regularize ultraviolet (UV) and infrared (IR) singularities in Dimensional Regularization (DR) (we write  $d = 4 - 2\epsilon$  and use an anticommuting  $\gamma_5$  according to the NDR scheme). In this case the SCET diagrams are

scaleless and vanish and the main task consists in the computation of the 2-loop QCD corrections to the left-hand side of (4). We parameterize the QCD result in terms of three form factors,

$$\langle u(p) | J^\mu | b(p_b) \rangle = \bar{u}(p) \left[ F_1(q^2) \gamma^\mu (1 - \gamma_5) + F_2(q^2) \frac{p_b^\mu}{m_b} (1 + \gamma_5) + F_3(q^2) \frac{p^\mu}{m_b} (1 + \gamma_5) \right] b(p_b), \quad (7)$$

with momentum transfer  $q = p_b - p$ . On the other hand we work in a frame with  $v = (n_- + n_+)/2$  and choose the basis of three independent Dirac structures in (4) as

$$\Gamma_1^\mu = \gamma^\mu (1 - \gamma_5), \quad \Gamma_2^\mu = v^\mu (1 + \gamma_5), \quad \Gamma_3^\mu = n_-^\mu (1 + \gamma_5). \quad (8)$$

Writing the momentum of the on-shell  $b$ -quark as  $p_b = m_b v$  and the one of the  $u$ -quark as  $p = (n_+ p) n_- / 2$  provides the link between the form factors  $F_i$  and the coefficient functions  $C_i$ . We finally introduce a dimensionless variable  $u$  to parameterize the light-cone momentum of the  $u$ -quark as  $u = n_+ p / m_b$ . In this notation the momentum transfer becomes  $q^2 = \bar{u} m_b^2$  with  $\bar{u} = 1 - u$ .

### 3. NNLO calculation of QCD form factors

#### 3.1. 2-loop calculation

To NNLO the QCD calculation of the form factors  $F_i(q^2)$  involves the calculation of the 2-loop diagrams from Fig. 1. As pointed out in the introduction, the calculation can be inferred from the calculation of the 2-loop vertex corrections to hadronic  $B$  decays [9]. The present calculation involves only a small subset of 2-loop diagrams and about half of the Master Integrals (MIs) that have been computed in [9].

The calculation follows the same strategy that has been used in [9]. We first express tensor integrals in terms of scalar integrals with the help of a general tensor decomposition. We then use an automatized reduction algorithm, which is based on integration-by-parts techniques [10] and the Laporta algorithm [11], to express the scalar integrals in terms of an irreducible set of Master Integrals (MIs). As long as we neglect the charm quark mass, the present calculation gives rise to 14 MIs which are depicted in Fig. 2. All MIs have already been calculated in [9] with the help of the method of differential equations [12], the formalism of Harmonic Polylogarithms (HPLs) [13], Mellin–Barnes techniques [14] and the method of sector decomposition [15].

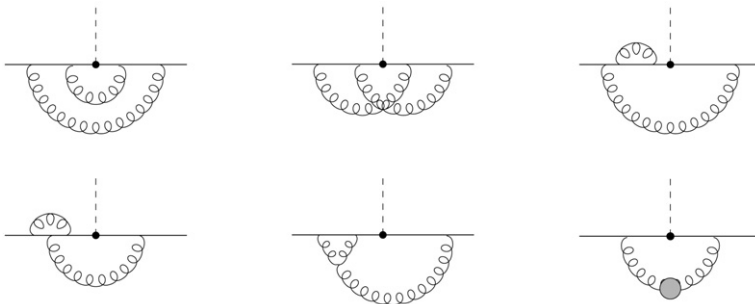


Fig. 1. 2-loop diagrams. Diagrams that result from mirroring at the vertical axis are not shown. The bubble in the last diagram represents the 1-loop gluon self-energy.

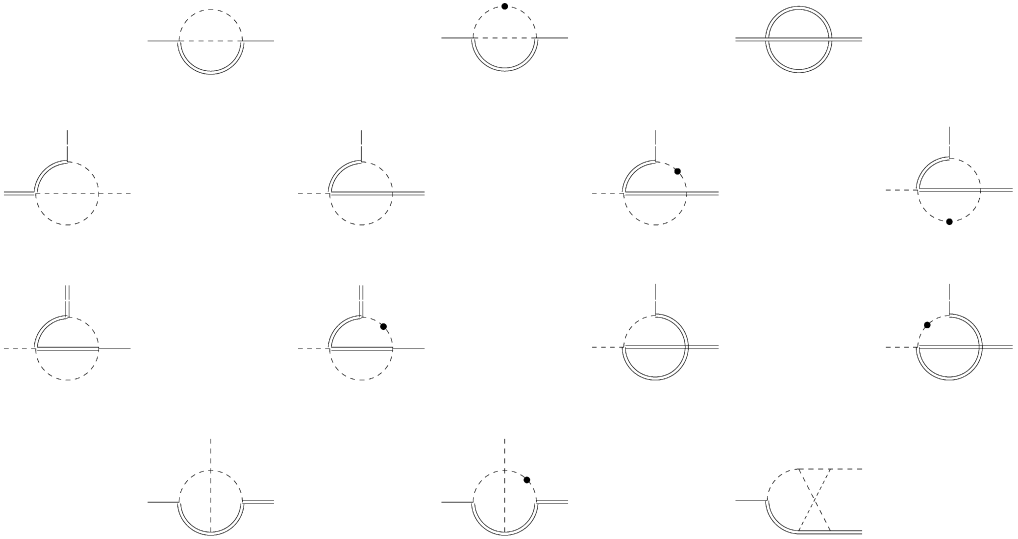


Fig. 2. Scalar 2-loop Master Integrals. We use dashed (double) lines for massless (massive) propagators. Dashed/solid/double external lines correspond to virtualities  $0/m_b^2/m_b^2$ , respectively. Dotted propagators are taken to be squared.

The MIs from Fig. 2 can be expressed in terms of HPLs of weight  $w \leq 4$ . Throughout this paper, we give our results in terms of the following minimal set of HPLs

$$\begin{aligned}
 H(0; x) &= \ln(x), & H(0, 0, 1; x) &= \text{Li}_3(x), \\
 H(1; x) &= -\ln(1-x), & H(0, 1, 1; x) &= \text{S}_{1,2}(x), \\
 H(-1; x) &= \ln(1+x), & H(0, 0, 0, 1; x) &= \text{Li}_4(x), \\
 H(0, 1; x) &= \text{Li}_2(x), & H(0, 0, 1, 1; x) &= \text{S}_{2,2}(x), \\
 H(0, -1; x) &= -\text{Li}_2(-x), & H(0, 1, 1, 1; x) &= \text{S}_{1,3}(x).
 \end{aligned}
 \tag{9}$$

Moreover, we introduce a shorthand notation for a HPL of weight  $w = 3$ , whose expression in terms of Nielsen Polylogarithms is rather involved

$$\begin{aligned}
 \mathcal{H}_1(x) &\equiv H(-1, 0, 1; x) \\
 &= \text{Li}_3\left(\frac{1-x}{2}\right) + \text{Li}_3\left(\frac{1-x}{1+x}\right) + \text{S}_{1,2}(x) + \text{S}_{1,2}(-x) - \text{S}_{1,2}\left(\frac{1-x}{2}\right) \\
 &\quad + \ln(1-x)\text{Li}_2(x) - \ln\left(\frac{1-x}{1+x}\right)\text{Li}_2(-x) - \ln\left(\frac{1+x}{2}\right)\text{Li}_2\left(\frac{1-x}{2}\right) \\
 &\quad - \frac{1}{6}\ln^3\left(\frac{1+x}{2}\right) + \frac{1}{2}\ln(x)\ln^2\left(\frac{1-x}{1+x}\right) - \frac{\pi^2}{4}\ln\left(\frac{1-x}{1+x}\right) - \frac{7}{4}\zeta_3,
 \end{aligned}
 \tag{10}$$

and for a HPL of weight  $w = 4$ , which cannot be expressed in terms of Nielsen Polylogarithms and has to be evaluated numerically,

$$\mathcal{H}_2(x) \equiv H(0, -1, 0, 1; x) = \int_0^x dx' \frac{\mathcal{H}_1(x')}{x'}.
 \tag{11}$$

The MIs from Fig. 2 have been computed in an analytic form [9], apart from a single number  $C_0$  which arises in the calculation of the boundary condition to the 6-topology MI (last diagram from Fig. 2). With the help of the MATHEMATICA package FIESTA [16], we can compute this number to higher precision than in [9]. We now find  $C_0 = -60.250 \pm 0.001$ .

### 3.2. Renormalization

The form factors, which we obtain from the 2-loop diagrams of Fig. 1, are UV- and IR-divergent. The UV-divergences are subtracted in the renormalization procedure which amounts to the calculation of several 1-loop diagrams with standard QCD counterterm insertions. We account for the wave-function renormalization of the quark fields by

$$F_i = Z_{2,u}^{1/2} Z_{2,b}^{1/2} F_{i,\text{bare}}, \tag{12}$$

where  $Z_{2,u}$  ( $Z_{2,b}$ ) is the wave-function renormalization factor of the massless  $u$ -quark (massive  $b$ -quark). Writing the perturbative expansion in terms of the renormalized coupling constant  $\alpha_s$ ,

$$F_{i,\text{(bare)}} = \sum_{k=0}^{\infty} \left( \frac{\alpha_s}{4\pi} \right)^k F_{i,\text{(bare)}}^{(k)}, \quad Z_{2,u/b} = 1 + \sum_{k=1}^{\infty} \left( \frac{\alpha_s}{4\pi} \right)^k Z_{2,u/b}^{(k)}, \tag{13}$$

we find that the renormalized form factors are given to NNLO by

$$\begin{aligned} F_i^{(0)} &= F_{i,\text{bare}}^{(0)}, \\ F_i^{(1)} &= F_{i,\text{bare}}^{(1)} + \frac{1}{2} (Z_{2,u}^{(1)} + Z_{2,b}^{(1)}) F_{i,\text{bare}}^{(0)}, \\ F_i^{(2)} &= F_{i,\text{bare}}^{(2)} + \frac{1}{2} (Z_{2,u}^{(1)} + Z_{2,b}^{(1)}) F_{i,\text{bare}}^{(1)} \\ &\quad + \left( \frac{1}{2} (Z_{2,u}^{(2)} + Z_{2,b}^{(2)}) - \frac{1}{8} (Z_{2,u}^{(1)} - Z_{2,b}^{(1)})^2 \right) F_{i,\text{bare}}^{(0)}. \end{aligned} \tag{14}$$

We renormalize the coupling constant in the  $\overline{\text{MS}}$ -scheme (adopting the notation (13))

$$Z_g^{(1)} = - \left( \frac{11}{6} C_A - \frac{2}{3} n_f T_F \right) \frac{1}{\epsilon}, \tag{15}$$

whereas the quark wave-functions and the  $b$ -quark mass are renormalized in the on-shell scheme,

$$Z_{2,b}^{(1)} = Z_m^{(1)} = -C_F \left( \frac{e^{\gamma_E} \mu^2}{m_b^2} \right)^\epsilon \Gamma(\epsilon) \frac{3 - 2\epsilon}{1 - 2\epsilon}, \tag{16}$$

and  $Z_{2,u}^{(1)} = 0$  because of the fact that scaleless integrals vanish in DR. According to (14), we also need the 2-loop expressions for the wave-function renormalization factors. For a massless quark  $Z_{2,u}^{(2)}$  can be calculated easily, since it receives a contribution from a single diagram, shown in Fig. 3, which introduces a mass scale. We find, in agreement with e.g. [23],

$$Z_{2,u}^{(2)} = T_F C_F \left( \frac{e^{\gamma_E} \mu^2}{m_b^2} \right)^{2\epsilon} \Gamma(\epsilon)^2 \frac{2\epsilon(3 - 2\epsilon)(1 + \epsilon)}{(1 - \epsilon)(2 - \epsilon)(1 + 2\epsilon)(3 + 2\epsilon)}. \tag{17}$$

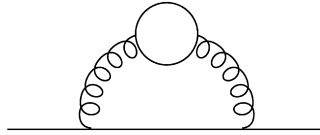


Fig. 3. 2-loop diagram with massive fermion loop.

For a massive quark  $Z_{2,b}^{(2)}$  has been calculated in [17],

$$\begin{aligned}
 Z_{2,b}^{(2)} = C_F & \left\{ \left[ \frac{9}{2} C_F + \frac{11}{2} C_A - 2n_l T_F \right] \frac{1}{\varepsilon^2} \right. \\
 & + \left[ \left( \frac{51}{4} + 9L \right) C_F - \frac{127}{12} C_A + \frac{11}{3} n_l T_F + (1 + 4L) T_F \right] \frac{1}{\varepsilon} \\
 & + \left( \frac{433}{8} - \frac{49\pi^2}{4} + 16\pi^2 \ln(2) - 24\zeta_3 + \frac{51}{2} L + 9L^2 \right) C_F \\
 & + \left( -\frac{1705}{24} + 5\pi^2 - 8\pi^2 \ln(2) + 12\zeta_3 - \frac{215}{6} L - \frac{11}{2} L^2 \right) C_A \\
 & + \left( \frac{113}{6} + \frac{4\pi^2}{3} + \frac{38}{3} L + 2L^2 \right) n_l T_F \\
 & \left. + \left( \frac{947}{18} - 5\pi^2 + \frac{22}{3} L + 6L^2 \right) T_F + \mathcal{O}(\varepsilon) \right\}, \tag{18}
 \end{aligned}$$

with  $L \equiv \ln \mu^2/m_b^2$  and the number of massless quarks  $n_l = 4$ .

### 3.3. Renormalized form factors

We now present our results for the renormalized form factors  $F_i(q^2)$ . It should be noticed that these form factors are formally IR divergent. We address the subtraction of these IR-divergences in the following section.

It will be convenient to further decompose the coefficients  $F_i^{(k)}$  of the perturbative expansion (13) according to

$$F_i^{(k)} = \sum_j F_{i,j}^{(k)} \varepsilon^j. \tag{19}$$

We suppress an overall prefactor  $ig_w V_{ub}/2\sqrt{2}$  and recall that  $q^2 = \bar{u}m_b^2$  with  $\bar{u} = 1 - u$  and  $L = \ln \mu^2/m_b^2$ . In our normalization the form factors become in leading order

$$F_1^{(0)}(u) = 1, \quad F_2^{(0)}(u) = 0, \quad F_3^{(0)}(u) = 0. \tag{20}$$

In NLO we give our result up to terms of  $\mathcal{O}(\varepsilon^2)$ , which are required for the IR-subtractions that we consider in the following section. In terms of a set of coefficient functions  $f_i(u)$ ,  $i = 1, \dots, 10$ , which we list in Appendix A, we find that the form factor  $F_1$  is given by

$$\begin{aligned}
 F_{1,-2}^{(1)}(u) &= -C_F, \\
 F_{1,-1}^{(1)}(u) &= C_F(f_1(u) - L),
 \end{aligned}$$

$$\begin{aligned}
F_{1,0}^{(1)}(u) &= C_F \left( f_2(u) + f_1(u)L - \frac{1}{2}L^2 \right), \\
F_{1,1}^{(1)}(u) &= C_F \left( f_3(u) + f_2(u)L + \frac{1}{2}f_1(u)L^2 - \frac{1}{6}L^3 \right), \\
F_{1,2}^{(1)}(u) &= C_F \left( f_4(u) + f_3(u)L + \frac{1}{2}f_2(u)L^2 + \frac{1}{6}f_1(u)L^3 - \frac{1}{24}L^4 \right),
\end{aligned} \tag{21}$$

whereas the other two form factors are finite at NLO and read

$$\begin{aligned}
F_{2,0}^{(1)}(u) &= C_F f_5(u), \\
F_{2,1}^{(1)}(u) &= C_F (f_6(u) + f_5(u)L), \\
F_{2,2}^{(1)}(u) &= C_F \left( f_7(u) + f_6(u)L + \frac{1}{2}f_5(u)L^2 \right),
\end{aligned} \tag{22}$$

and

$$\begin{aligned}
F_{3,0}^{(1)}(u) &= C_F f_8(u), \\
F_{3,1}^{(1)}(u) &= C_F (f_9(u) + f_8(u)L), \\
F_{3,2}^{(1)}(u) &= C_F \left( f_{10}(u) + f_9(u)L + \frac{1}{2}f_8(u)L^2 \right).
\end{aligned} \tag{23}$$

In NNLO the divergent terms of the form factors can also be expressed in terms of the 1-loop coefficient functions  $f_i(u)$ . The divergent terms of the form factor  $F_1$  read

$$\begin{aligned}
F_{1,-4}^{(2)}(u) &= \frac{1}{2}C_F^2, \\
F_{1,-3}^{(2)}(u) &= C_F^2(L - f_1(u)) + \frac{11}{4}C_A C_F - n_l T_F C_F, \\
F_{1,-2}^{(2)}(u) &= C_F^2 \left[ L^2 - 2f_1(u)L + \frac{1}{2}f_1(u)^2 - f_2(u) \right] + C_A C_F \left[ \frac{11}{6}(L - f_1(u)) \right. \\
&\quad \left. - \frac{67}{36} + \frac{\pi^2}{12} \right] + n_l T_F C_F \left[ \frac{5}{9} - \frac{2}{3}(L - f_1(u)) \right] + \frac{4}{3}L T_F C_F, \\
F_{1,-1}^{(2)}(u) &= C_F^2 \left[ \frac{2}{3}L^3 - 2f_1(u)L^2 - (2f_2(u) - f_1(u)^2)L + f_1(u)f_2(u) - f_3(u) - \frac{3}{8} \right. \\
&\quad \left. + \frac{\pi^2}{2} - 6\zeta_3 \right] + C_A C_F \left[ \left( \frac{\pi^2}{6} - \frac{67}{18} \right) (L - f_1(u)) + \frac{461}{216} - \frac{17\pi^2}{24} + \frac{11}{2}\zeta_3 \right] \\
&\quad + n_l T_F C_F \left[ \frac{10}{9}(L - f_1(u)) - \frac{25}{54} + \frac{\pi^2}{6} \right] + T_F C_F \left[ 2L^2 - \frac{4}{3}f_1(u)L + \frac{\pi^2}{9} \right],
\end{aligned} \tag{24}$$

whereas the other two form factors start with a  $1/\varepsilon^2$ -singularity,

$$\begin{aligned}
F_{2,-2}^{(2)}(u) &= -C_F^2 f_5(u), \\
F_{2,-1}^{(2)}(u) &= C_F^2 (f_1(u)f_5(u) - f_6(u) - 2f_5(u)L),
\end{aligned} \tag{25}$$



and

$$\begin{aligned}
 F_{3,-2}^{(2)}(u) &= -C_F^2 f_8(u), \\
 F_{3,-1}^{(2)}(u) &= C_F^2 (f_1(u) f_8(u) - f_9(u) - 2f_8(u)L). \tag{26}
 \end{aligned}$$

The finite terms of the 2-loop form factors give rise to a new set of coefficient functions  $k_i(u)$ ,  $i = 1, \dots, 10$ , which we collect in [Appendix B](#). We find

$$\begin{aligned}
 F_{1,0}^{(2)}(u) &= C_F^2 \left[ \frac{1}{3} L^4 - \frac{4}{3} f_1(u) L^3 - (2f_2(u) - f_1(u)^2) L^2 - \left( 2f_3(u) - 2f_2(u)f_1(u) + \frac{3}{4} \right. \right. \\
 &\quad \left. \left. - \pi^2 + 12\zeta_3 \right) L + k_1(u) \right] + C_A C_F \left[ -\frac{11}{18} L^3 + \left( \frac{11}{6} f_1(u) - \frac{67}{18} + \frac{\pi^2}{6} \right) L^2 \right. \\
 &\quad \left. + \left( \frac{11}{3} f_2(u) + \left( \frac{67}{9} - \frac{\pi^2}{3} \right) f_1(u) + \frac{461}{108} - \frac{17\pi^2}{12} + 11\zeta_3 \right) L + k_2(u) \right] \\
 &\quad + n_l T_F C_F \left[ \frac{2}{9} L^3 - \left( \frac{2}{3} f_1(u) - \frac{10}{9} \right) L^2 - \left( \frac{4}{3} f_2(u) + \frac{20}{9} f_1(u) + \frac{25}{27} - \frac{\pi^2}{3} \right) L \right. \\
 &\quad \left. - \frac{4}{3} f_3(u) - \frac{20}{9} f_2(u) + \left( \frac{25}{27} - \frac{\pi^2}{3} \right) f_1(u) + k_3(u) \right] \\
 &\quad + T_F C_F \left[ \frac{14}{9} L^3 - 2f_1(u) L^2 - \left( \frac{4}{3} f_2(u) - \frac{2\pi^2}{9} \right) L + k_4(u) \right], \\
 F_{2,0}^{(2)}(u) &= C_F^2 [k_5(u) + 2(f_1(u) f_5(u) - f_6(u))L - 2f_5(u)L^2] \\
 &\quad + C_A C_F \left[ k_6(u) + \frac{11}{3} f_5(u)L \right] \\
 &\quad + n_l T_F C_F \left[ -\frac{4}{3} f_6(u) - \frac{14}{9} f_5(u) - \frac{4}{3} f_5(u)L \right] + T_F C_F \left[ k_7(u) - \frac{4}{3} f_5(u)L \right], \\
 F_{3,0}^{(2)}(u) &= C_F^2 [k_8(u) + 2(f_1(u) f_8(u) - f_9(u))L - 2f_8(u)L^2] + C_A C_F \left[ k_9(u) \right. \\
 &\quad \left. + \frac{11}{3} f_8(u)L \right] + n_l T_F C_F \left[ \frac{8}{3\bar{u}} \ln(u) - \frac{4}{3} f_9(u) - \frac{14}{9} f_8(u) - \frac{4}{3} f_8(u)L \right] \\
 &\quad + T_F C_F \left[ k_{10}(u) - \frac{4}{3} f_8(u)L \right]. \tag{27}
 \end{aligned}$$

We compared our results for the 2-loop form factors with the ones given in [\[8\]](#) and found complete analytical agreement.

## 4. Matching calculation

### 4.1. IR-subtractions

In order to extract the Wilson coefficients  $C_i$  from the form factors  $F_i$  of the previous section, we have to consider the perturbative expansion of the hadronic tensor  $W^{\mu\nu}$  and to absorb the IR-singularities of the form factors into the jet function  $J$  and the shape function  $S$ . As the convolution of jet and shape function is independent from the indices  $(i, j)$  it is convenient to

rewrite the factorization formula (6) as  $W^{\mu\nu} = \sum c_{ij}^{\mu\nu} W_{ij}$  with

$$W_{ij} = C_i C_j J \otimes S, \quad (28)$$

where the symbol  $\otimes$  represents the convolution integral. When we write the perturbative expansion in terms of the renormalized coupling constant, we should keep in mind that the actual 2-loop calculation has been performed in QCD with five active quark flavours, while the NNLO calculation of the jet function [7] and the partonic shape function [18] have been performed in SCET with four active flavours. We therefore have to account for an additional finite renormalization to consistently express the perturbative expansion in terms of the renormalized coupling constant of the four-flavour theory,

$$\alpha_s^{(5)}(\mu) = \alpha_s^{(4)}(\mu) \left[ 1 + \frac{\alpha_s^{(4)}(\mu)}{4\pi} \delta\alpha_s^{(1)} + \mathcal{O}(\alpha_s^2) \right], \quad (29)$$

with (cf. e.g. [19])

$$\delta\alpha_s^{(1)} = T_F \left[ \frac{4}{3}L + \left( \frac{2}{3}L^2 + \frac{\pi^2}{9} \right) \varepsilon + \left( \frac{2}{9}L^3 + \frac{\pi^2}{9}L - \frac{4}{9}\zeta_3 \right) \varepsilon^2 + \mathcal{O}(\varepsilon^3) \right]. \quad (30)$$

In the four-flavour theory the perturbative expansion of the hadronic tensor becomes

$$\begin{aligned} W_{ij}^{(0)} &= C_i^{(0)} C_j^{(0)} [J \otimes S]^{(0)}, \\ W_{ij}^{(1)} &= (C_i^{(1)} C_j^{(0)} + C_i^{(0)} C_j^{(1)}) [J \otimes S]^{(0)} + C_i^{(0)} C_j^{(0)} [J \otimes S]^{(1)}, \\ W_{ij}^{(2)} &= (C_i^{(2)} C_j^{(0)} + C_i^{(1)} C_j^{(1)} + C_i^{(0)} C_j^{(2)} - \delta\alpha_s^{(1)} C_i^{(1)} C_j^{(0)} - \delta\alpha_s^{(1)} C_i^{(0)} C_j^{(1)}) [J \otimes S]^{(0)} \\ &\quad + (C_i^{(1)} C_j^{(0)} + C_i^{(0)} C_j^{(1)} - \delta\alpha_s^{(1)} C_i^{(0)} C_j^{(0)}) [J \otimes S]^{(1)} + C_i^{(0)} C_j^{(0)} [J \otimes S]^{(2)}. \end{aligned} \quad (31)$$

As we have mentioned in Section 2, the matching calculation simplifies in our setup due to the fact that the SCET diagrams are scaleless and vanish. The IR-subtractions are therefore entirely determined by the counterterms. At NLO the counterterm can be inferred from [6]. In terms of the coefficient function  $f_1(u)$  from Appendix A, it reads

$$[J \otimes S]^{(1)} = C_F \left\{ -\frac{2}{\varepsilon^2} - \frac{2}{\varepsilon} (L - f_1(u)) \right\} [J \otimes S]^{(0)}. \quad (32)$$

In NNLO the counterterm can be extracted from the analysis in [7,18]. We obtain

$$\begin{aligned} [J \otimes S]^{(2)} &= C_F \left\{ \frac{2C_F}{\varepsilon^4} + \left[ 4(L - f_1(u))C_F + \frac{11}{2}C_A - 2n_l T_F \right] \frac{1}{\varepsilon^3} \right. \\ &\quad + \left[ (2L^2 - 4f_1(u)L + 2f_1(u)^2)C_F + \left( \frac{\pi^2}{6} - \frac{67}{18} + \frac{11}{3}(L - f_1(u)) \right) C_A \right. \\ &\quad + \left. \left( \frac{10}{9} - \frac{4}{3}(L - f_1(u)) \right) n_l T_F \right] \frac{1}{\varepsilon^2} + \left[ \left( \pi^2 - \frac{3}{4} - 12\zeta_3 \right) C_F \right. \\ &\quad + \left. \left( \frac{461}{108} - \frac{17\pi^2}{12} + 11\zeta_3 + \left( \frac{\pi^2}{3} - \frac{67}{9} \right) (L - f_1(u)) \right) C_A \right. \\ &\quad + \left. \left. \left( \frac{\pi^2}{3} - \frac{25}{27} + \frac{20}{9}(L - f_1(u)) \right) n_l T_F \right] \frac{1}{\varepsilon} \right\} [J \otimes S]^{(0)}. \end{aligned} \quad (33)$$

#### 4.2. Hard coefficient functions in NNLO

We now have assembled all pieces required for the NNLO calculation of the hard coefficient functions  $H_{ij}$ . Performing the IR-subtractions as described in the previous section, we observe that the UV- and IR-divergences cancel in the hard coefficient functions which represents both a non-trivial confirmation of the factorization formula (6) and a stringent cross-check of our calculation.

We give the results for the hard coefficient functions in terms of the Wilson coefficients  $C_i$ , which arise in the matching relation (4) of the heavy-to-light current,  $H_{ij} = C_i C_j$ . We remind that the perturbative expansion is formulated in terms of the renormalized coupling constant in a four-flavour theory and that in leading order

$$C_1^{(0)}(u) = 1, \quad C_2^{(0)}(u) = 0, \quad C_3^{(0)}(u) = 0. \quad (34)$$

In NLO we obtain in terms of our results from Section 3.3,

$$\begin{aligned} C_1^{(1)}(u) &= F_{1,0}^{(1)}(u), \\ C_2^{(1)}(u) &= F_{2,0}^{(1)}(u), \\ \frac{2}{u} C_3^{(1)}(u) &= F_{3,0}^{(1)}(u). \end{aligned} \quad (35)$$

The NNLO coefficient functions were so far unknown. They are found in this work to be

$$\begin{aligned} C_1^{(2)}(u) &= F_{1,0}^{(2)} + T_F C_F \left[ \frac{4}{9} \zeta_3 + \frac{\pi^2}{9} f_1(u) + \frac{2}{9} (6f_2(u) - \pi^2)L + 2f_1(u)L^2 - \frac{14}{9}L^3 \right] \\ &\quad + C_F^2 \left[ f_4(u) - f_1(u)f_3(u) + (2f_3(u) - f_1(u)f_2(u))L \right. \\ &\quad \left. + \frac{1}{2} (3f_2(u) - f_1(u)^2)L^2 + \frac{5}{6} f_1(u)L^3 - \frac{5}{24}L^4 \right], \end{aligned} \quad (36)$$

and

$$\begin{aligned} C_2^{(2)}(u) &= F_{2,0}^{(2)} + T_F C_F \left[ \frac{4}{3} f_5(u)L \right] \\ &\quad + C_F^2 \left[ f_7(u) - f_1(u)f_6(u) + (2f_6(u) - f_1(u)f_5(u))L + \frac{3}{2} f_5(u)L^2 \right], \end{aligned} \quad (37)$$

and

$$\begin{aligned} \frac{2}{u} C_3^{(2)}(u) &= F_{3,0}^{(2)} + T_F C_F \left[ \frac{4}{3} f_8(u)L \right] \\ &\quad + C_F^2 \left[ f_{10}(u) - f_1(u)f_9(u) + (2f_9(u) - f_1(u)f_8(u))L + \frac{3}{2} f_8(u)L^2 \right]. \end{aligned} \quad (38)$$

The hard functions  $H_{ij}$  and hence the Wilson coefficients  $C_i$  are renormalization scale dependent. According to the factorization formula (6), this scale dependence has to cancel against the one of the convolution of jet and shape function. The scale dependence of the Wilson coefficients  $C_i$  is governed by the renormalization group equation,

$$\frac{d}{d \ln \mu} C_i(u; \mu) = \left[ \Gamma_{\text{cusp}}(\alpha_s) \ln \frac{um_b}{\mu} + \gamma'(\alpha_s) \right] C_i(u; \mu), \quad (39)$$

where  $\Gamma_{\text{cusp}}$  is the universal cusp anomalous dimension which describes the renormalization properties of light-like Wilson lines [20]. Writing the perturbative expansion as

$$\Gamma_{\text{cusp}}(\alpha_s) = \sum_{k=1}^{\infty} \left( \frac{\alpha_s}{4\pi} \right)^k \Gamma_{\text{cusp}}^{(k)}, \quad \gamma'(\alpha_s) = \sum_{k=1}^{\infty} \left( \frac{\alpha_s}{4\pi} \right)^k \gamma'^{(k)}, \quad (40)$$

we derive from our NLO expressions in (35) the familiar results

$$\Gamma_{\text{cusp}}^{(1)} = 4C_F, \quad \gamma'^{(1)} = -5C_F. \quad (41)$$

Similarly, we can read off from our NNLO results (36)–(38) that

$$\begin{aligned} \Gamma_{\text{cusp}}^{(2)} &= C_A C_F \left[ \frac{268}{9} - \frac{4\pi^2}{3} \right] - \frac{80}{9} n_l T_F C_F, \\ \gamma'^{(2)} &= C_F^2 \left[ 2\pi^2 - \frac{3}{2} - 24\zeta_3 \right] + C_A C_F \left[ 22\zeta_3 - \frac{1549}{54} - \frac{7\pi^2}{6} \right] \\ &\quad + n_l T_F C_F \left[ \frac{250}{27} + \frac{2\pi^2}{3} \right]. \end{aligned} \quad (42)$$

While our result for the 2-loop cusp anomalous dimension is in agreement with [20], the expression for  $\gamma'^{(2)}$  has not yet been computed directly so far. Our result confirms the conjecture in [21], which was based on known results of the 2-loop anomalous dimensions of the jet and the shape function.

## 5. Charm mass effects

In this section we extend our analysis to include charm mass effects. The charm quark enters the 2-loop calculation through the 1-loop gluon self energy in the last diagram of Fig. 1. So far we treated the charm quark as massless and the respective effects are given in the above formulas by the terms that are proportional to  $n_l = 4$ , which denotes the number of massless quarks.

A comment is in order about the power counting of the charm quark mass within the effective theory approach. One possible choice is given by  $m_c \sim \mu_{hc} \sim (\Lambda_{\text{QCD}} m_b)^{1/2}$ , i.e. the additional mass scale is considered to be of the order of the intermediate hard-collinear scale. In this case charm mass effects enter in the calculation of the jet function. In this setup the charm mass represents an IR-scale in the QCD  $\rightarrow$  SCET matching calculation and can therefore be set to zero. If we adopt the scaling  $m_c \sim \mu_{hc}$ , the hard coefficient functions  $H_{ij}$  are thus given by the formulas from Section 4.

A second choice, which has been widely applied in studies of  $b \rightarrow c$  decays, is to consider the charm quark in the heavy quark limit with  $m_b \rightarrow \infty$  and  $m_c \rightarrow \infty$  while  $m_c/m_b$  is kept fixed. In this scenario the hard coefficient functions  $H_{ij}$  depend on the mass ratio  $z = m_c/m_b$ . On the other hand the jet function does not depend on the charm quark mass in this setup, since it is defined in SCET with three active quark flavours. Both approaches differ in the fact that the first one allows to resum logarithms of the form  $\ln m_c/m_b$  while the second one does not.

In the following we consider the second scenario, i.e. we keep a finite charm quark mass in the 2-loop QCD calculation and the subsequent matching calculation. We briefly outline the steps of the calculation that change when we introduce a finite charm quark mass and write our results schematically as (for an arbitrary quantity  $\mathcal{Q}$ )

$$\mathcal{Q}(z) = \hat{\mathcal{Q}} + \Delta \mathcal{Q}(z), \quad (43)$$



Fig. 4. Additional Master Integrals with propagators of mass  $m_c$  (wavy line). Notation as in Fig. 2.

where  $\hat{Q}$  refers to the respective expression from Section 3 or 4 but with  $n_l = 3$  massless quark flavours and  $\Delta Q(z)$  gives the additional contribution from a massive charm quark.

### 5.1. QCD form factors

The charm mass enters the QCD calculation through the 2-loop diagram with a closed charm quark loop, which gives rise to four additional MIs (depicted in Fig. 4). Since these MIs have not been considered in [9], we present our results for these MIs in Appendix C. As discussed in the appendix, we obtain analytical results apart from the finite terms of the 4-topology MIs. We could, however, find suitable representations which allow us to evaluate these terms numerically to very high precision. Moreover, we provide compact parameterizations for physical values of  $z = m_c/m_b$  in the appendix, which reproduce our numerical results at the percent level.

The charm mass also modifies the renormalization procedure. We get an additional contribution to the 2-loop wave-function renormalization factor of the  $u$ -quark,

$$\Delta Z_{2,u}^{(2)}(z) = T_F C_F \left( \frac{e^{\gamma_E} \mu^2}{z^2 m_b^2} \right)^{2\varepsilon} \Gamma(\varepsilon)^2 \frac{2\varepsilon(3-2\varepsilon)(1+\varepsilon)}{(1-\varepsilon)(2-\varepsilon)(1+2\varepsilon)(3+2\varepsilon)}, \quad (44)$$

whereas the one of the  $b$ -quark receives the additional contribution [17],

$$\begin{aligned} \Delta Z_{2,b}^{(2)}(z) = T_F C_F \left\{ (1 + 4L_c) \frac{1}{\varepsilon} + 6L_c^2 + \left( \frac{22}{3} + 8 \ln(z) \right) L_c \right. \\ + \frac{(5 - 18z - 30z^3 + 12z^4)\pi^2}{3} + \frac{4}{3} (19 + 12z^2) \ln(z) + 8(1 + 3z^4) \ln^2(z) \\ - 8z(3 + 5z^2) (\text{Li}_2(-z) + \ln(z) \ln(1+z)) \\ - 2(1-z)(2-z-z^2-6z^3) (\text{Li}_2(z^2) + 2 \ln(z) \ln(1-z^2)) \\ \left. + \frac{443}{18} + 28z^2 + \mathcal{O}(\varepsilon) \right\}, \quad (45) \end{aligned}$$

where we introduced  $L_c = \ln \mu^2/m_c^2 = L - 2 \ln(z)$ .

These changes modify our NNLO expressions for the renormalized QCD form factors  $F_i(q^2)$  from Section 3.3. We now introduce three additional coefficient functions  $k_i(u, z)$ ,  $i = 11, \dots, 13$ , which we list in Appendix B. The form factor  $F_1$  receives the additional contribution

$$\begin{aligned} \Delta F_{1,-2}^{(2)}(u, z) &= \frac{4}{3} L_c T_F C_F, \\ \Delta F_{1,-1}^{(2)}(u, z) &= \left[ 2L_c^2 - \frac{4}{3} (f_1(u) - 2 \ln(z)) L_c + \frac{\pi^2}{9} \right] T_F C_F, \end{aligned}$$

$$\begin{aligned} \Delta F_{1,-0}^{(2)}(u, z) = & \left[ \frac{14}{9} L_c^3 - 2(f_1(u) - 2\ln(z)) L_c^2 \right. \\ & - \frac{4}{3} \left( f_2(u) + 2\ln(z) f_1(u) - 2\ln^2(z) - \frac{\pi^2}{6} \right) L_c \\ & \left. + k_{11}(u, z) \right] T_F C_F, \end{aligned} \quad (46)$$

whereas the other two form factors are modified by

$$\begin{aligned} \Delta F_{2,0}^{(2)}(u, z) &= \left[ k_{12}(u, z) - \frac{4}{3} f_5(u) L_c \right] T_F C_F, \\ \Delta F_{3,0}^{(2)}(u, z) &= \left[ k_{13}(u, z) - \frac{4}{3} f_8(u) L_c \right] T_F C_F. \end{aligned} \quad (47)$$

## 5.2. Hard coefficient functions

According to the power counting that we adopt for the charm quark mass scale, the charm quark is integrated out in the QCD  $\rightarrow$  SCET matching calculation. The IR-subtractions turn out to be analogous to those of Section 4.1, apart from the fact that we now match onto SCET with three active quark flavours. If we express the perturbative expansion in terms of the renormalized coupling constant of the three-flavour theory, we thus have to account for an additional contribution to (29) with

$$\Delta \delta \alpha_s^{(1)}(z) = T_F \left[ \frac{4}{3} L_c + \left( \frac{2}{3} L_c^2 + \frac{\pi^2}{9} \right) \varepsilon + \left( \frac{2}{9} L_c^3 + \frac{\pi^2}{9} L_c - \frac{4}{9} \zeta_3 \right) \varepsilon^2 + \mathcal{O}(\varepsilon^3) \right], \quad (48)$$

where we recall that  $L_c = \ln \mu^2 / m_c^2 = L - 2\ln(z)$ .

We summarize our results for the hard coefficient functions  $H_{ij} = C_i C_j$ . If we keep a finite charm quark mass in the matching calculation, which corresponds to the power counting  $m_b \rightarrow \infty$  and  $m_c \rightarrow \infty$  with  $m_c/m_b$  fixed, we find that the coefficients functions are given in NNLO by our results from (36)–(38) with  $n_l = 3$  massless quarks and the additional contributions

$$\begin{aligned} \Delta C_1^{(2)}(u, z) &= \left[ k_{11}(u, z) + (f_1(u) - 2\ln(z)) \frac{\pi^2}{9} + \frac{4}{9} \zeta_3 \right] T_F C_F, \\ \Delta C_2^{(2)}(u, z) &= k_{12}(u, z) T_F C_F, \\ \frac{2}{u} \Delta C_3^{(2)}(u, z) &= k_{13}(u, z) T_F C_F, \end{aligned} \quad (49)$$

which depend on the quark mass ratio  $z = m_c/m_b$ .

## 6. Numerical analysis

We briefly discuss the numerical impact of the considered NNLO corrections. As a phenomenological analysis of inclusive semileptonic  $B$  decays is beyond the scope of the present paper, we illustrate our results at the level of the Wilson coefficients  $C_i$  which arise in the match-

ing relation (4) of the semileptonic current (recall that the hard coefficient functions from (6) are given by  $H_{ij} = C_i C_j$ ). We in particular do not study the renormalization scale dependence, since the Wilson coefficients are explicitly scale dependent, cf. (39). The scale dependence is cancelled only at the level of the hadronic tensor against the one of the jet and the shape function.

In Fig. 5 we show the Wilson coefficients  $C_i$  at the scale  $\mu = m_b$ . We see that the considered NNLO corrections give moderate contributions to the Wilson coefficients, which add constructively to the NLO corrections. The effect of the finite charm quark mass is small, but amounts to  $\sim 10$ – $20\%$  of the NNLO contribution as can be seen in Fig. 6. In Fig. 6 we also illustrate a scenario, which considers the charm quark to be as heavy as the  $b$ -quark, i.e.  $z = m_c/m_b = 1$  (dashed line). Somewhat surprising, the curves for physical charm masses with  $z \simeq 0.3$  are much closer to the limit  $m_c = m_b$  than to the limit  $m_c = 0$  (notice that the effect is even slightly larger for physical charm masses than for  $m_c = m_b$ ).

## 7. Conclusion

We computed NNLO corrections to the hard coefficient functions  $H_{ij}$  which arise in the factorization formula (6) for inclusive semileptonic  $B$  meson decays in the shape-function region. Together with the 2-loop corrections to the jet function from [7], our calculation completes the NNLO calculation of  $B \rightarrow X_u \ell \nu$  decays in the shape-function region.

The considered calculation is closely related to the 2-loop calculation in charmless hadronic  $B$  decays [9]. In particular, all Master Integrals that appear in the present calculation have already been calculated in [9]. We confirmed analytical results for the 2-loop form factors which have been computed recently in [8] and extended the analysis to extract the hard coefficient functions  $H_{ij}$  from the form factors which are formally IR-divergent. We in addition kept a finite charm quark mass in the 2-loop calculation.

A phenomenological analysis of partial decay rates in the shape-function region was beyond the scope of the present paper. We briefly discussed the numerical impact of the considered corrections to the short-distance coefficients, which was found to be moderate. One should keep in mind, however, that the present calculation reflects only a part of the full NNLO calculation. We in particular expect that the renormalization scale dependence of the theoretical prediction for partial decay rates will be significantly reduced, once the renormalization group improvement is taken into account in NNLO.

### Note added

While this paper was in preparation, the work in [22,23] on the same topic appeared. While the analysis in [23] did not go beyond the one in [8], the authors of [22] also performed the full matching calculation. We have compared our results for the NNLO hard coefficient functions from (36)–(38) with those in [22] and found agreement. None of the works in [22,23] addressed charm mass effects.

## Acknowledgements

We are grateful to Gerhard Buchalla for many interesting discussions and comments on the manuscript. We thank Roberto Bonciani and Andrea Ferroglia for discussions related to the 6-topology Master Integral. This work was supported by the DFG Sonderforschungsbereich/Transregio 9.

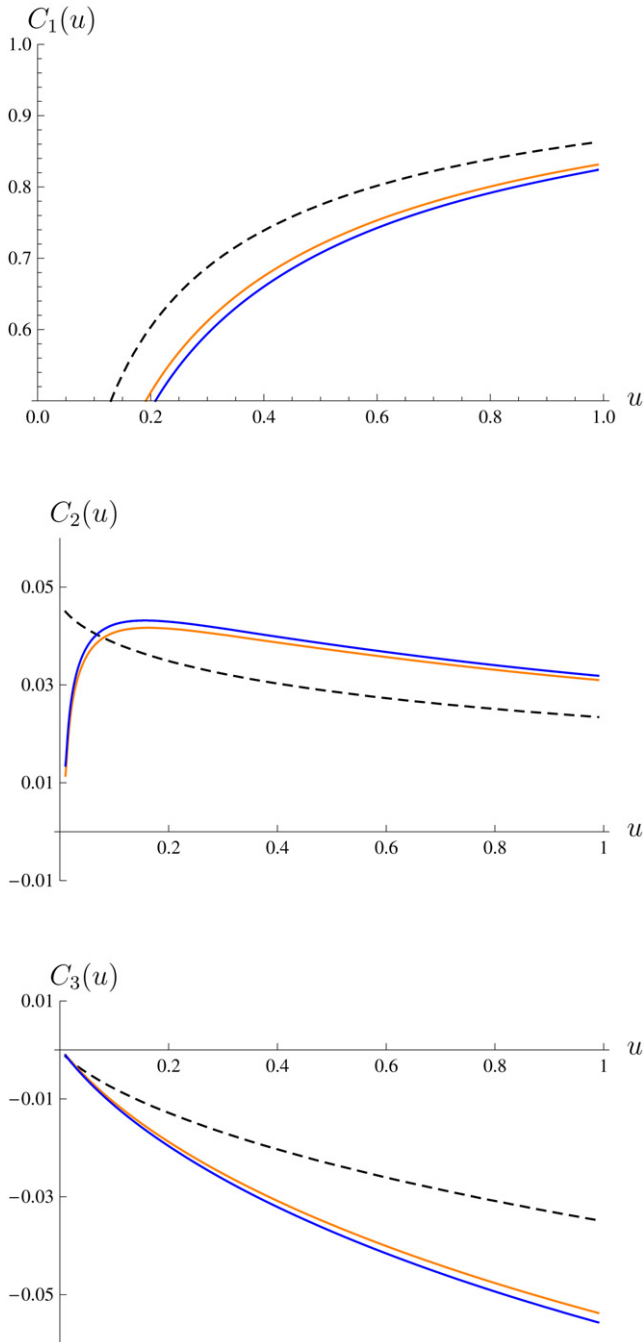


Fig. 5. Wilson coefficients  $C_i$  at the scale  $\mu = m_b$  as a function of  $u$  (the momentum transfer is given by  $q^2 = (1-u)m_b^2$ ). The dashed lines refer to the NLO results and the solid lines to the NNLO results with  $z = m_c/m_b = 0$  (orange/light gray) and  $z = 0.3$  (blue/dark gray). (For interpretation of the references to colour in this figure legend, the reader is referred to the web version of this paper.)



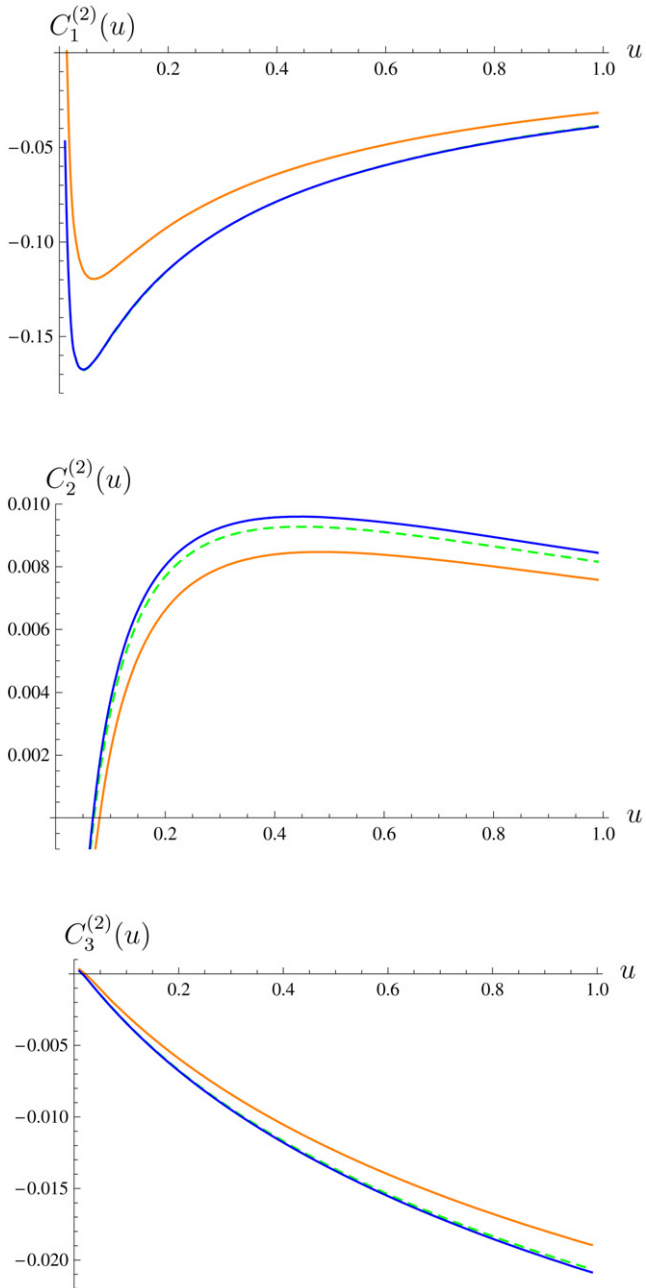


Fig. 6. NNLO contributions to the Wilson coefficients  $C_i$  at the scale  $\mu = m_b$  as a function of  $u$ . The solid lines again refer to the NNLO results with  $z = m_c/m_b = 0$  (orange/light gray) and  $z = 0.3$  (blue/dark gray). The dashed green/light gray line shows the limit  $z = 1$ . In the first and the third plot the dashed line can hardly be distinguished from the solid blue/dark gray line. (For interpretation of the references to colour in this figure legend, the reader is referred to the web version of this paper.)

## Appendix A. NLO coefficient functions

The 1-loop calculation of the QCD form factors gives rise to the following coefficient functions

$$\begin{aligned}
 f_1(u) &= -\frac{5}{2} + 2 \ln(u), \\
 f_2(u) &= -6 - \frac{\pi^2}{12} - \frac{1-3\bar{u}}{\bar{u}} \ln(u) - 2 \ln^2(u) - 2 \text{Li}_2(\bar{u}), \\
 f_3(u) &= -12 - \frac{5\pi^2}{24} + \frac{1}{3} \zeta_3 - \frac{24(1-2\bar{u}) - \pi^2 \bar{u}}{6\bar{u}} \ln(u) + \frac{1-3\bar{u}}{\bar{u}} (\ln^2(u) + \text{Li}_2(\bar{u})) \\
 &\quad + \frac{4}{3} \ln^3(u) + 4 \ln(u) \text{Li}_2(\bar{u}) - 2 \text{Li}_3(\bar{u}) + 4 \text{S}_{1,2}(\bar{u}), \\
 f_4(u) &= -24 - \frac{\pi^2}{2} - \frac{\pi^4}{160} + \frac{5}{6} \zeta_3 - \frac{96(1-2\bar{u}) + (1-3\bar{u})\pi^2 + 8\bar{u}\zeta_3}{12\bar{u}} \ln(u) \\
 &\quad + \frac{24(1-2\bar{u}) - \pi^2 \bar{u}}{6\bar{u}} (\ln^2(u) + \text{Li}_2(\bar{u})) - \frac{2}{3} \ln^4(u) - 4 \ln^2(u) \text{Li}_2(\bar{u}) \\
 &\quad - \frac{1-3\bar{u}}{\bar{u}} \left( \frac{2}{3} \ln^3(u) + 2 \ln(u) \text{Li}_2(\bar{u}) - \text{Li}_3(\bar{u}) + 2 \text{S}_{1,2}(\bar{u}) \right) - 8 \ln(u) \text{S}_{1,2}(\bar{u}) \\
 &\quad + 4 \ln(u) \text{Li}_3(\bar{u}) - 2 \text{Li}_4(\bar{u}) - 8 \text{S}_{1,3}(\bar{u}) + 4 \text{S}_{2,2}(\bar{u}), \\
 f_5(u) &= \frac{2}{\bar{u}} + \frac{2u}{\bar{u}^2} \ln(u), \\
 f_6(u) &= \frac{4}{\bar{u}} + \frac{2u}{\bar{u}^2} (\ln(u) - \ln^2(u) - \text{Li}_2(\bar{u})), \\
 f_7(u) &= \frac{48 + \pi^2}{6\bar{u}} + \frac{2u}{\bar{u}^2} \left( \frac{24 + \pi^2}{12} \ln(u) - \ln^2(u) - \text{Li}_2(\bar{u}) + \frac{2}{3} \ln^3(u) + 2 \ln(u) \text{Li}_2(\bar{u}) \right. \\
 &\quad \left. - \text{Li}_3(\bar{u}) + 2 \text{S}_{1,2}(\bar{u}) \right), \\
 f_8(u) &= -\frac{2}{\bar{u}} - \frac{2(1-2\bar{u})}{\bar{u}^2} \ln(u), \\
 f_9(u) &= -\frac{4}{\bar{u}} - \frac{2(1-5\bar{u})}{\bar{u}^2} \ln(u) + \frac{2(1-2\bar{u})}{\bar{u}^2} (\ln^2(u) + \text{Li}_2(\bar{u})), \\
 f_{10}(u) &= -\frac{48 + \pi^2}{6\bar{u}} - \frac{24(1-5\bar{u}) + \pi^2(1-2\bar{u})}{6\bar{u}^2} \ln(u) + \frac{2(1-5\bar{u})}{\bar{u}^2} (\ln^2(u) + \text{Li}_2(\bar{u})) \\
 &\quad - \frac{2(1-2\bar{u})}{\bar{u}^2} \left( \frac{2}{3} \ln^3(u) + 2 \ln(u) \text{Li}_2(\bar{u}) - \text{Li}_3(\bar{u}) + 2 \text{S}_{1,2}(\bar{u}) \right). \tag{A.1}
 \end{aligned}$$

## Appendix B. NNLO coefficient functions

In the 2-loop expressions of the QCD form factors (27) we introduced the coefficient functions  $k_i(u)$ , which read

$$k_1(u) = \frac{2(5 + 31\bar{u} + 3\bar{u}^2 + 3\bar{u}^3)}{u^3} \text{Li}_4(\bar{u}) + \frac{4(13 + 53\bar{u} + 15\bar{u}^2 + 3\bar{u}^3)}{u^3} \text{S}_{2,2}(\bar{u}) + 8 \text{S}_{1,3}(\bar{u})$$

$$\begin{aligned}
& - \frac{2(3 + 14\bar{u} + 3\bar{u}^2 + \bar{u}^3)}{u^3} \text{Li}_2(\bar{u})^2 - 8 \ln(u) \text{Li}_3(\bar{u}) + 16 \ln(u) \text{S}_{1,2}(\bar{u}) + \frac{16}{3} \ln^4(u) \\
& + 16 \ln^2(u) \text{Li}_2(\bar{u}) + \frac{3 + 100\bar{u} + 145\bar{u}^2 + 4\bar{u}^3}{3u^2\bar{u}} \text{Li}_3(\bar{u}) + \frac{42 - 68\bar{u}}{9\bar{u}} \ln^3(u) \\
& - \frac{2(3 - 242\bar{u} - 233\bar{u}^2 - 32\bar{u}^3)}{3u^2\bar{u}} \text{S}_{1,2}(\bar{u}) + \frac{2(6 + 41\bar{u} + 77\bar{u}^2 + 2\bar{u}^3)}{3u^2\bar{u}} \ln(u) \text{Li}_2(\bar{u}) \\
& - \left( \frac{3 + 89\bar{u} + 785\bar{u}^2 + 635\bar{u}^3}{18u^2\bar{u}} + \frac{(5 + 31\bar{u} + 3\bar{u}^2 + 3\bar{u}^3)\pi^2}{u^3} \right) \text{Li}_2(\bar{u}) \\
& - \left( \frac{147 - 736\bar{u} - 167\bar{u}^2}{18u\bar{u}} - 2\pi^2 \right) \ln^2(u) - \frac{(5267 + 10490\bar{u} + 2387\bar{u}^2)\pi^2}{432u^2} \\
& - \left( \frac{291 - 959\bar{u}}{54\bar{u}} - \frac{(9 + 340\bar{u} + 355\bar{u}^2 + 52\bar{u}^3)\pi^2}{18u^2\bar{u}} + \frac{56}{3} \zeta_3 \right) \ln(u) \\
& + \frac{(787 + 2607\bar{u} + 1065\bar{u}^2 + 77\bar{u}^3)\pi^4}{720u^3} + \frac{67}{9} \zeta_3 - \frac{71387}{1296} - 2k_2(u), \\
k_2(u) = & - \frac{4(1 - 3\bar{u} + \bar{u}^2 + 5\bar{u}^3)}{12u^2\bar{u}} (12\mathcal{H}_1(\bar{u}) + \pi^2 \ln(2 - u)) + \frac{8(1 + 2\bar{u} + 4\bar{u}^2)}{u^3} \text{S}_{2,2}(\bar{u}) \\
& - \frac{2\bar{u} - u^3}{3u^3} (24\mathcal{H}_2(\bar{u}) - 2\pi^2 \text{Li}_2(-\bar{u})) \\
& + \frac{2(1 + 10\bar{u} + 4\bar{u}^2)}{u^3} \text{Li}_4(\bar{u}) - 8 \ln(u) \text{Li}_3(\bar{u}) \\
& - \frac{5 - 10\bar{u} + 16\bar{u}^2 - 4\bar{u}^3}{u^3} \text{Li}_2(\bar{u})^2 + \frac{8 + 36\bar{u} - 33\bar{u}^2 - 20\bar{u}^3}{3u^3} \text{Li}_3(\bar{u}) \\
& + \frac{92 - 24\bar{u} - 33\bar{u}^2 - 26\bar{u}^3}{3u^3} \text{S}_{1,2}(\bar{u}) + \frac{47 - 49\bar{u} + 44\bar{u}^2}{3u^2} \ln(u) \text{Li}_2(\bar{u}) + \frac{44}{9} \ln^3(u) \\
& + \left( \frac{33 - 227\bar{u} + 157\bar{u}^2 - 116\bar{u}^3}{9u^2\bar{u}} + \frac{(1 - 26\bar{u} - 4\bar{u}^3)\pi^2}{3u^3} \right) \text{Li}_2(\bar{u}) \\
& + \frac{39 - 235\bar{u} + 349\bar{u}^2 + 12u\bar{u}\pi^2}{18u\bar{u}} \ln^2(u) - \frac{(419 + 1178\bar{u} + 815\bar{u}^2)\pi^2}{216u^2} \\
& - \left( \frac{807 - 2545\bar{u}}{54\bar{u}} - \frac{(12 + 65\bar{u} + 41\bar{u}^2 + 56\bar{u}^3)\pi^2}{18u^2\bar{u}} + 14\zeta_3 \right) \ln(u) + \frac{289 - 19\bar{u}}{18u} \zeta_3 \\
& + \frac{u^2 - 3}{u^3} \left( \text{Li}_3(-u) - \ln(u) \text{Li}_2(-u) - \frac{\ln^2(u) + \pi^2}{2} \ln(1 + u) \right) - \frac{89437}{1296} \\
& - \frac{(227 - 1935\bar{u} + 519\bar{u}^2 - 389\bar{u}^3)\pi^4}{1080u^3} - \frac{(6 + 2\bar{u})\pi^2}{u} \ln(2) - \mathcal{C}_0, \\
k_3(u) = & - \frac{10}{3\bar{u}} \ln(u) - \frac{2125}{324} + \frac{5\pi^2}{18} + \frac{10}{3} \zeta_3, \\
k_4(u) = & \frac{8(6\bar{u} + u^3)}{3u^3} \text{Li}_3(\bar{u}) - \frac{4(3 + 8\bar{u} - 24\bar{u}^3 - 19\bar{u}^4)}{9u^3\bar{u}} \text{Li}_2(\bar{u}) - \frac{144\bar{u} + 28u^3}{9u^3} \zeta_3 \\
& + \frac{2(57 + 89\bar{u} - 73\bar{u}^2 - 265\bar{u}^3 - 3\bar{u}u^2\pi^2)}{27u^2\bar{u}} \ln(u)
\end{aligned}$$

$$\begin{aligned}
& + \frac{(23 + 315\bar{u} - 507\bar{u}^2 + 41\bar{u}^3)\pi^2}{54u^3} + \frac{1111 - 6758\bar{u} + 7951\bar{u}^2}{162u^2}, \\
k_5(u) = & \frac{4(13 + 8\bar{u})}{u^3} (2\text{Li}_4(\bar{u}) + 8\text{S}_{2,2}(\bar{u}) - \text{Li}_2(\bar{u})^2 - \pi^2 \text{Li}_2(\bar{u})) + \frac{262 - 298\bar{u}}{9\bar{u}^2} \ln(u) \\
& - \frac{1 - 15\bar{u} - 67\bar{u}^2 - 3\bar{u}^3}{u^2\bar{u}^2} (2\text{Li}_3(\bar{u}) + \pi^2 \ln(u)) \\
& + \frac{4(1 + 21\bar{u} + 143\bar{u}^2 + 3\bar{u}^3)}{u^2\bar{u}^2} \text{S}_{1,2}(\bar{u}) \\
& - \frac{4(2 - 12\bar{u} - 29\bar{u}^2 - 3\bar{u}^3)}{u^2\bar{u}^2} \ln(u) \text{Li}_2(\bar{u}) - \frac{5 - 171\bar{u} + 507\bar{u}^2 + 163\bar{u}^3}{3u^2\bar{u}^2} \text{Li}_2(\bar{u}) \\
& - \frac{28u}{3\bar{u}^2} \ln^3(u) + \frac{12 - 41\bar{u} + 190\bar{u}^2 + 91\bar{u}^3}{3u\bar{u}^3} \ln^2(u) - \frac{(3 + 214\bar{u} + 35\bar{u}^2)\pi^2}{3u^2\bar{u}} \\
& + \frac{3(13 + 8\bar{u})\pi^4}{5u^3} + \frac{259}{9\bar{u}} - 2k_6(u), \\
k_6(u) = & \frac{2(1 - 3\bar{u} - 3\bar{u}^2 + \bar{u}^3)}{3u^2\bar{u}^2} (12\mathcal{H}_1(\bar{u}) + \pi^2 \ln(2 - u)) \\
& - \frac{4}{3u^3} (24\mathcal{H}_2(\bar{u}) - 2\pi^2 \text{Li}_2(-\bar{u})) \\
& + \frac{4(11 + 4\bar{u})}{u^3} \text{Li}_4(\bar{u}) + \frac{2(3 + 4\bar{u})}{u^3} (8\text{S}_{2,2}(\bar{u}) - \text{Li}_2(\bar{u})^2) - \frac{13 - 56\bar{u} - 8\bar{u}^2}{3u\bar{u}^2} \ln^2(u) \\
& + \frac{2(2 + 30\bar{u} - 38\bar{u}^2 + 3\bar{u}^3)}{u^3\bar{u}} \text{Li}_3(\bar{u}) + \frac{2(8 + 36\bar{u} - 30\bar{u}^2 - 11\bar{u}^3)}{u^3\bar{u}} \text{S}_{1,2}(\bar{u}) \\
& + \frac{2(2 + 9\bar{u} + 3\bar{u}^2)}{u^2\bar{u}} \ln(u) \text{Li}_2(\bar{u}) - \frac{(6 + 53\bar{u} + 8\bar{u}^2)\pi^2}{3u^2\bar{u}} + \frac{269}{9\bar{u}} \\
& - \left( \frac{2(11 - 45\bar{u} + 60\bar{u}^2 + 25\bar{u}^3)}{3u^2\bar{u}^2} + \frac{2(17 + 12\bar{u})\pi^2}{3u^3} \right) \text{Li}_2(\bar{u}) - \frac{2(7 + \bar{u})}{u^2} \zeta_3 \\
& + \left( \frac{203 - 257\bar{u}}{9\bar{u}^2} - \frac{(4 - 18\bar{u} - 39\bar{u}^2 - 5\bar{u}^3)\pi^2}{3u^2\bar{u}^2} \right) \ln(u) + \frac{(155 + 108\bar{u})\pi^4}{90u^3} \\
& - \frac{2(8 - 6\bar{u} + \bar{u}^2)}{u^3} \left( \text{Li}_3(-u) - \ln(u) \text{Li}_2(-u) - \frac{\ln^2(u) + \pi^2}{2} \ln(1 + u) \right), \\
k_7(u) = & \frac{32}{u^3} \text{Li}_3(\bar{u}) + \frac{8(1 - 3\bar{u} - 3\bar{u}^2 + \bar{u}^3)}{3u^2\bar{u}^2} \text{Li}_2(\bar{u}) - \frac{4(13 - 86\bar{u} + 13\bar{u}^2)}{9u\bar{u}^2} \ln(u) \\
& + \frac{32(3 - \bar{u})\pi^2}{9u^2} - \frac{32}{u^3} \zeta_3 - \frac{4(19 + 59\bar{u})}{9u\bar{u}}, \\
k_8(u) = & - \frac{4(19 + 32\bar{u} + 12\bar{u}^2)}{u^4} (2\text{Li}_4(\bar{u}) + 8\text{S}_{2,2}(\bar{u}) - \text{Li}_2(\bar{u})^2 - \pi^2 \text{Li}_2(\bar{u})) \\
& + \frac{1 - 17\bar{u} - 129\bar{u}^2 - 101\bar{u}^3 - 6\bar{u}^4}{u^3\bar{u}^2} (2\text{Li}_3(\bar{u}) + \pi^2 \ln(u)) + \frac{28(1 - 2\bar{u})}{3\bar{u}^2} \ln^3(u) \\
& - \frac{4(1 + 19\bar{u} + 285\bar{u}^2 + 181\bar{u}^3 + 18\bar{u}^4)}{u^3\bar{u}^2} \text{S}_{1,2}(\bar{u}) - \frac{3(19 + 32\bar{u} + 12\bar{u}^2)\pi^4}{5u^4} \\
& + \frac{4(2 - 16\bar{u} - 51\bar{u}^2 - 61\bar{u}^3)}{u^3\bar{u}^2} \ln(u) \text{Li}_2(\bar{u}) + \frac{(3 + 323\bar{u} + 373\bar{u}^2 + 57\bar{u}^3)\pi^2}{3u^3\bar{u}}
\end{aligned}$$

$$\begin{aligned}
 & + \frac{5 - 187\bar{u} + 363\bar{u}^2 + 1123\bar{u}^3 + 208\bar{u}^4}{3u^3\bar{u}^2} \text{Li}_2(\bar{u}) - \frac{262 - 771\bar{u} + 149\bar{u}^2}{9u\bar{u}^2} \ln(u) \\
 & - \frac{12 - 53\bar{u} + 182\bar{u}^2 + 587\bar{u}^3 + 28\bar{u}^4}{3u^2\bar{u}^3} \ln^2(u) - \frac{259 - 151\bar{u}}{9u\bar{u}} - 2k_9(u), \\
 k_9(u) = & - \frac{2(1 - 5\bar{u} - 5\bar{u}^2 - \bar{u}^3 - 2\bar{u}^4)}{3u^3\bar{u}^2} (12\mathcal{H}_1(\bar{u}) + \pi^2 \ln(2 - u)) \\
 & + \frac{4(1 + 2\bar{u})}{3u^4} (24\mathcal{H}_2(\bar{u}) - 2\pi^2 \text{Li}_2(-\bar{u})) - \frac{4(13 + 24\bar{u} + 8\bar{u}^2)}{u^4} \text{Li}_4(\bar{u}) \\
 & - \frac{2(5 + 8\bar{u} + 8\bar{u}^2)}{u^4} (8\text{S}_{2,2}(\bar{u}) - \text{Li}_2(\bar{u})^2) \\
 & - \frac{2(2 + 48\bar{u} - 28\bar{u}^2 - 25\bar{u}^3 - 6\bar{u}^4)}{u^4\bar{u}} \text{Li}_3(\bar{u}) \\
 & - \frac{2(8 + 70\bar{u} + 16\bar{u}^2 - 71\bar{u}^3 - 14\bar{u}^4)}{u^4\bar{u}} \text{S}_{1,2}(\bar{u}) + \frac{13 - 82\bar{u} - 34\bar{u}^2 - 50\bar{u}^3}{3u^2\bar{u}^2} \ln^2(u) \\
 & - \frac{2(2 + 17\bar{u} + 17\bar{u}^2 + 6\bar{u}^3)}{u^3\bar{u}} \ln(u) \text{Li}_2(\bar{u}) + \frac{(6 + 103\bar{u} + 60\bar{u}^2 + 32\bar{u}^3)\pi^2}{3u^3\bar{u}} \\
 & + \left( \frac{2(11 - 67\bar{u} + 72\bar{u}^2 + 103\bar{u}^3 + 34\bar{u}^4)}{3u^3\bar{u}^2} + \frac{2(23 + 40\bar{u} + 24\bar{u}^2)\pi^2}{3u^4} \right) \text{Li}_2(\bar{u}) \\
 & - \left( \frac{203 - 795\bar{u} + 430\bar{u}^2}{9u\bar{u}^2} - \frac{(4 - 26\bar{u} - 47\bar{u}^2 - 103\bar{u}^3 - 2\bar{u}^4)\pi^2}{3u^3\bar{u}^2} \right) \ln(u) \\
 & + \frac{2(22 - 20\bar{u} + 9\bar{u}^2 - 2\bar{u}^3)}{u^4} \left( \text{Li}_3(-u) - \ln(u) \text{Li}_2(-u) \right. \\
 & \left. - \frac{\ln^2(u) + \pi^2}{2} \ln(1 + u) \right) \\
 & + \frac{2(23 - 17\bar{u} + 10\bar{u}^2)}{u^3} \zeta_3 - \frac{(209 + 364\bar{u} + 216\bar{u}^2)\pi^4}{90u^4} \\
 & - \frac{8\pi^2}{u} \ln(2) - \frac{269 - 215\bar{u}}{9u\bar{u}}, \\
 k_{10}(u) = & - \frac{32(1 + 2\bar{u})}{u^4} (\text{Li}_3(\bar{u}) - \zeta_3) - \frac{8(1 - 5\bar{u} - 21\bar{u}^2 - 17\bar{u}^3 - 2\bar{u}^4)}{3u^3\bar{u}^2} \text{Li}_2(\bar{u}) \\
 & + \frac{4(13 - 124\bar{u} - 223\bar{u}^2 - 38\bar{u}^3)}{9u^2\bar{u}^2} \ln(u) - \frac{16(15 + 4\bar{u} + \bar{u}^2)\pi^2}{9u^3} \\
 & + \frac{4(19 + 364\bar{u} + 43\bar{u}^2)}{9u^2\bar{u}}. \tag{B.1}
 \end{aligned}$$

The definition of the functions  $\mathcal{H}_{1,2}(x)$  and the constant  $\mathcal{C}_0$  can be found in Section 3.1.

When we include a finite charm quark mass in our calculation, we encounter three additional coefficient functions which depend on the quark mass ratio  $z = m_c/m_b$ . They have been introduced in (46) and (47) and read

$$\begin{aligned}
 & k_{11}(u, z) \\
 & = \frac{4(u^3 + 6\bar{u}z^4)}{3u^2z^2} \mathcal{I}_1(\bar{u}, z) + \frac{4(3u^4 - (3 - 19\bar{u})u^2z^2 - 4(3 - 7\bar{u})\bar{u}z^4)}{9u(1 + \bar{u})z^2} \mathcal{I}_2(\bar{u}, z)
 \end{aligned}$$

$$\begin{aligned}
 & + \left( \frac{24u^3(1-z) - (49 + 119\bar{u} + 175\bar{u}^2 - 55\bar{u}^3)z^5 - 18(1+\bar{u})(1-8\bar{u}+3\bar{u}^2)z^6}{9u^2(1+\bar{u})z^2} \right. \\
 & + \left. \frac{(69 - 80\bar{u} + 27\bar{u}^2)uz^3 + 4(15 - 2\bar{u} + 23\bar{u}^2)z^4 - 2(31 - 13\bar{u})u^2z^2}{9u^2(1+\bar{u})z^2} \right) \\
 & \times (\text{Li}_2(z^2) + 2\ln(z)\ln(1-z^2)) \\
 & + \frac{4((3 - 19\bar{u})u^2 + 2(15 - 23\bar{u})\bar{u}z^2)}{9u^2\bar{u}} (\text{Li}_2(\bar{u}) + \ln^2(u)) \\
 & + \frac{4(24u^3 - (69 - 80\bar{u} + 27\bar{u}^2)uz^2 + (49 + 119\bar{u} + 175\bar{u}^2 - 55\bar{u}^3)z^4)}{9u^2(1+\bar{u})z} \\
 & \times (\text{Li}_2(-z) + \ln(z)\ln(1+z)) - \frac{2(54u^3 - (21 - (37 + 3\pi^2)\bar{u})uz^2 + 216\bar{u}z^4)}{27u\bar{u}z^2} \ln(u) \\
 & - \frac{4(12u^4 - (37 - 51\bar{u})u^2z^2 + 2(15 - 32u\bar{u} + \bar{u}^2)z^4 - 9(1 - 8\bar{u} + 3\bar{u}^2)(1 + \bar{u})z^6)}{9u^2(1+\bar{u})z^2} \ln^2(z) \\
 & - \frac{2(72u^3 - (469 + 3\pi^2 - (59 - 3\pi^2)\bar{u})uz^2 + 12(29 + 3\bar{u} + 14\bar{u}^2)z^4)}{27u(1+\bar{u})z^2} \ln(z) - \frac{4}{9}\zeta_3 \\
 & - \frac{(12(7 - \bar{u})u^3 - 144u^3z + 40(3 - \bar{u} + 12\bar{u}^2)z^4 - 36(1 + \bar{u})(1 - 8\bar{u} + 3\bar{u}^2)z^6)\pi^2}{54u^2(1+\bar{u})z^2} \\
 & - \frac{(6(69 - 80\bar{u} + 27\bar{u}^2)uz^3 - (163 - 189\bar{u})u^2z^2 - 6(49 + 119\bar{u} + 175\bar{u}^2 - 55\bar{u}^3)z^5)\pi^2}{54u^2(1+\bar{u})z^2} \\
 & - \frac{108(27 + 11\bar{u})u^3 - (5827 - 509\bar{u})u^2z^2 + 36(107 + 265\bar{u} + 395\bar{u}^2 - 83\bar{u}^3)z^4}{162u^2(1+\bar{u})z^2} \\
 & + \frac{8((3 - 19\bar{u})u^2 + 2(15 - 23\bar{u})\bar{u}z^2)}{9u^2\bar{u}} \ln(z)\ln(u), \\
 k_{12}(u, z) & = \frac{16z^2}{u^2} \mathcal{I}_1(\bar{u}, z) + \frac{8(u^2 + 4\bar{u}z^2)}{3\bar{u}(1+\bar{u})} \mathcal{I}_2(\bar{u}, z) - \frac{8(u^2 - 2\bar{u}z^2)}{3u\bar{u}^2} (\text{Li}_2(\bar{u}) + \ln^2(u)) \\
 & + \frac{8(u^3 - 2u^2z + (1 + 10\bar{u} + \bar{u}^2)z^2 - 4(5 + 2\bar{u} - \bar{u}^2)\bar{u}z^3 + 3(1 + \bar{u})(3 - \bar{u})\bar{u}z^4)}{3u^2\bar{u}(1+\bar{u})} \\
 & \times (\text{Li}_2(z^2) + 2\ln(z)\ln(1-z^2)) - \frac{16((3 - \bar{u})u + (13 + 5\bar{u})\bar{u}z^2)}{3u\bar{u}(1+\bar{u})} \ln(z) \\
 & + \frac{64(u^2z + 2(5 + 2\bar{u} - \bar{u}^2)\bar{u}z^3)}{3u^2\bar{u}(1+\bar{u})} (\text{Li}_2(-z) + \ln(z)\ln(1+z)) \\
 & - \frac{16(2u^3 + (1 + 9\bar{u})uz^2 + 3(1 + \bar{u})(3 - \bar{u})\bar{u}z^4)}{3u^2\bar{u}(1+\bar{u})} \ln^2(z) - \frac{4(u^2 + 72\bar{u}z^2)}{9u\bar{u}^2} \ln(u) \\
 & - \frac{8(2u^3 - 6u^2z + (1 + 17\bar{u})z^2 - 12(5 + 2\bar{u} - \bar{u}^2)\bar{u}z^3 + 3(1 + \bar{u})(3 - \bar{u})\bar{u}z^4)\pi^2}{9u^2\bar{u}(1+\bar{u})} \\
 & - \frac{16(u^2 - 2\bar{u}z^2)}{3u\bar{u}^2} \ln(z)\ln(u) - \frac{4((43 - 5\bar{u})u^2 + 6(86 + 41\bar{u} - 13\bar{u}^2)\bar{u}z^2)}{9u^2\bar{u}(1+\bar{u})},
 \end{aligned}$$

$$\begin{aligned}
 k_{13}(u, z) &= \frac{16(3u^3 + (37 + 15\bar{u} + 2\bar{u}^2)\bar{u}z^2)}{3u^2\bar{u}(1 + \bar{u})} \ln(z) - \frac{16(1 + 2\bar{u})z^2}{u^3} \mathcal{I}_1(\bar{u}, z) \\
 &\quad - \frac{8(1 - 2\bar{u})(u^2 + 4\bar{u}z^2)}{3u\bar{u}(1 + \bar{u})} \mathcal{I}_2(\bar{u}, z) - \frac{16((1 - 2u)u^2 + 2(1 + 10\bar{u})\bar{u}z^2)}{3u^2\bar{u}^2} \ln(z) \ln(u) \\
 &\quad - \frac{32((2 - \bar{u} + 3\bar{u}^2)u^2z + (35 + 25\bar{u} + 13\bar{u}^2 - \bar{u}^3)\bar{u}z^3)}{3u^3\bar{u}(1 + \bar{u})} \\
 &\quad \times (\text{Li}_2(-z) + \ln(z) \ln(1 + z)) + \frac{8((1 - 2\bar{u})u^2 - 2(1 + 10\bar{u})\bar{u}z^2)}{3u^2\bar{u}^2} (\text{Li}_2(\bar{u}) + \ln^2(u)) \\
 &\quad + \frac{16(2(1 - 2\bar{u})u^3 + (1 + 19\bar{u} - 6\bar{u}^2)uz^2 + 3(1 + \bar{u})(5 + \bar{u})\bar{u}z^4)}{3u^3\bar{u}(1 + \bar{u})} \ln^2(z) \\
 &\quad - \frac{8(1 - z)^2((1 - 2\bar{u})u^3 - (5 - \bar{u})u^2\bar{u}z + 3(1 + \bar{u})(5 + \bar{u})\bar{u}z^2)}{3u^3\bar{u}(1 + \bar{u})} \\
 &\quad \times (\text{Li}_2(z^2) + 2\ln(z) \ln(1 - z^2)) \\
 &\quad + \frac{4((43 - 29\bar{u})u^3 + 6(140 + 127\bar{u} + 79\bar{u}^2 - 4\bar{u}^3)\bar{u}z^2)}{9u^3\bar{u}(1 + \bar{u})} \\
 &\quad + \frac{8(2(1 - 2\bar{u})u^3 - 3(2 - \bar{u} + 3\bar{u}^2)u^2z + (1 + 27\bar{u} + 2\bar{u}^2 + 24\bar{u}^3)z^2)\pi^2}{9u^3\bar{u}(1 + \bar{u})} \\
 &\quad - \frac{8(3(35 + 25\bar{u} + 13\bar{u}^2 - \bar{u}^3)z^3 - 3(1 + \bar{u})(5 + \bar{u})z^4)\pi^2}{9u^3(1 + \bar{u})} \\
 &\quad + \frac{4((1 - 14\bar{u})u^2 + 72(1 + 2\bar{u})\bar{u}z^2)}{9u^2\bar{u}^2} \ln(u), \tag{B.2}
 \end{aligned}$$

with the finite terms of the 4-topology MIs  $\mathcal{I}_{1,2}(u, z)$  that we introduced in Appendix C.

### Appendix C. Master Integrals

In this appendix we present our results for the MIs that involve the charm quark mass. The MIs are normalized according to

$$[dk] \equiv \frac{\Gamma(1 - \varepsilon)}{i\pi^{d/2}} d^d k \tag{C.1}$$

with  $d = 4 - 2\varepsilon$ . We suppress the  $+i\varepsilon$ -prescription of the particle propagators,

$$\begin{aligned}
 \mathcal{P}_1 &= (k - l)^2 - z^2 m_b^2, & \mathcal{P}_3 &= (p + k)^2 - m_b^2, \\
 \mathcal{P}_2 &= l^2 - z^2 m_b^2, & \mathcal{P}_4 &= (\bar{u}q + k)^2,
 \end{aligned} \tag{C.2}$$

and write  $z = m_c/m_b$  and  $\bar{u} = 1 - u$ .

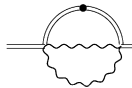
#### 3-topologies

$$\begin{aligned}
 \text{Diagram} &= \int [dk][dl] \frac{1}{\mathcal{P}_1 \mathcal{P}_2 \mathcal{P}_3} \equiv (m^2)^{1-2\varepsilon} \left\{ \sum_{i=-2}^1 d_i^{(31)} \varepsilon^i + \mathcal{O}(\varepsilon^2) \right\} \tag{C.3}
 \end{aligned}$$

with

$$\begin{aligned}
 d_{-2}^{(31)} &= \frac{1}{2} + z^2, \\
 d_{-1}^{(31)} &= \frac{5}{4} + 3z^2 - 4z^2 \ln(z), \\
 d_0^{(31)} &= \frac{11}{8} + 6z^2 + 2z^2((2 + z^2) \ln(z) - 7) \ln(z) + \frac{(3 - 2z^2 + 2z^4)\pi^2}{6} \\
 &\quad - (1 - z^2)^2 (\text{Li}_2(z^2) + 2 \ln(z) \ln(1 - z^2)), \\
 d_1^{(31)} &= -\frac{55}{16} + \frac{15}{2} z^2 - \frac{z^2}{3} ((8 + 12z^2) \ln^2(z) - 3(12 + 5z^2) \ln(z) + (111 + 4\pi^2)) \ln(z) \\
 &\quad + 2(1 - z^2)^2 [2\mathcal{H}_1(z) + \text{S}_{1,2}(z^2) + \ln(1 - z^2) \text{Li}_2(z^2) + 2 \ln(1 - z) \text{Li}_2(-z) \\
 &\quad + (2 \ln^2(1 - z^2) - \ln^2(1 - z) - \ln^2(1 + z)) \ln(z) - \pi^2 \ln(1 + z) + 2\zeta_3] \\
 &\quad + 8z(1 + z^2) (\text{Li}_2(-z) + \ln(z) \ln(1 + z)) + \frac{(15 + 24z - 24z^2 + 24z^3 + 10z^4)\pi^2}{12} \\
 &\quad - \frac{1}{2} (1 - z)^2 (5 + 14z + 5z^2) (\text{Li}_2(z^2) + 2 \ln(z) \ln(1 - z^2)), \tag{C.4}
 \end{aligned}$$

and the function  $\mathcal{H}_1(x)$  from Section 3.1.



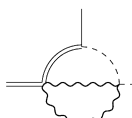
$$= \int [dk][dl] \frac{1}{\mathcal{P}_1 \mathcal{P}_2 \mathcal{P}_3^2} \equiv (m^2)^{-2\epsilon} \left\{ \sum_{i=-2}^1 d_i^{(32)} \epsilon^i + \mathcal{O}(\epsilon^2) \right\} \tag{C.5}$$

with

$$\begin{aligned}
 d_{-2}^{(32)} &= \frac{1}{2}, \\
 d_{-1}^{(32)} &= \frac{1}{2}, \\
 d_0^{(32)} &= -\frac{1}{2} - 2z^2 \ln^2 z - (1 - z^2) (\text{Li}_2(z^2) + 2 \ln(z) \ln(1 - z^2)) + \frac{(3 - 2z^2)\pi^2}{6}, \\
 d_1^{(32)} &= -\frac{11}{2} + 2z^2 (2 \ln(z) - 3) \ln^2(z) + \frac{(1 + 4z - 2z^2)\pi^2}{2} \\
 &\quad + 2(1 - z^2) [2\mathcal{H}_1(z) + \text{S}_{1,2}(z^2) + \ln(1 - z^2) \text{Li}_2(z^2) + 2 \ln(1 - z) \text{Li}_2(-z) \\
 &\quad + 8z (\text{Li}_2(-z) + \ln(z) \ln(1 + z)) - (1 - z)(1 + 3z) (\text{Li}_2(z^2) + 2 \ln(z) \ln(1 - z^2)) \\
 &\quad + (2 \ln^2(1 - z^2) - \ln^2(1 - z) - \ln^2(1 + z)) \ln(z) - \pi^2 \ln(1 + z) + 2\zeta_3]. \tag{C.6}
 \end{aligned}$$

4-topologies

The 4-topology MIs are complicated since they depend on three scales ( $um_b^2, m_c^2, m_b^2$ ). The divergent terms of the MIs are simple,



$$\begin{aligned}
 &= \int [dk][dl] \frac{1}{\mathcal{P}_1 \mathcal{P}_2 \mathcal{P}_3 \mathcal{P}_4} \\
 &= (m^2)^{-2\epsilon} \left\{ \frac{1}{2\epsilon^2} + \left( \frac{5}{2} + \frac{\bar{u}}{u} \ln(\bar{u}) \right) \frac{1}{\epsilon} + \mathcal{I}_1(u, z) + \mathcal{O}(\epsilon) \right\}, \tag{C.7}
 \end{aligned}$$

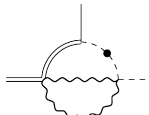


Table 1

Numerical input for the parameterizations (C.9) of the finite terms of the 4-topology Master Integrals.

$z$	$c_0$	$c_1$	$\rho$	$d_0$	$u_0$	$\sigma$	$\tau$
0.250	11.9022	0.9512	0.6575	13.1958	1.0164	0.2077	1.2244
0.275	11.5770	0.9053	0.6544	12.3101	1.0171	0.2170	1.2271
0.300	11.2538	0.8523	0.6506	11.5442	1.0177	0.2256	1.2295
0.325	10.9330	0.7934	0.6463	10.8767	1.0182	0.2335	1.2317
0.350	10.6147	0.7293	0.6414	10.2786	1.0187	0.2412	1.2339

and



$$\begin{aligned}
 &= \int [dk][dl] \frac{1}{\mathcal{P}_1 \mathcal{P}_2 \mathcal{P}_3 \mathcal{P}_4^2} \\
 &= (m^2)^{-1-2\epsilon} \left\{ \frac{1}{\bar{u}\epsilon^2} - \left( 2\ln(z) + \frac{1+u}{u} \ln(\bar{u}) \right) \frac{1}{\bar{u}\epsilon} \right. \\
 &\quad \left. + \mathcal{I}_2(u, z) + \mathcal{O}(\epsilon) \right\}, \tag{C.8}
 \end{aligned}$$

but we could not find analytical expressions for the finite terms  $\mathcal{I}_{1,2}(u, z)$ .<sup>1</sup> Unfortunately, a power expansion in  $z = m_c/m_b$  cannot be applied for the given MIs, since it generates powers of  $z/(1-u)$  which invalidate the expansion for large values of  $u$ .

We could, however, derive suitable one-dimensional Mellin–Barnes representations, which allow us to evaluate the finite terms numerically to very high precision. We use this representation for our numerical estimate of charm mass effects in Section 6, but also provide compact parameterizations which are in any case convenient since we expect the exact expressions to be rather involved. We propose the parameterizations

$$\begin{aligned}
 \mathcal{I}_1(u, z) &\simeq \frac{c_0 - c_1 u}{1 + (1-u)^\rho}, \\
 \mathcal{I}_2(u, z) &\simeq \frac{d_0}{(u_0 - u)^\sigma (1-u)^\tau}, \tag{C.9}
 \end{aligned}$$

which reproduce our numerical results over the entire  $u$ -range,  $0 < u < 1$ , and for physical values of  $z = m_c/m_b$  at the percent level. The numerical values of the parameters ( $c_0, c_1, \rho, \dots$ ) depend on the value of  $z$  and can be found in Table 1.

**References**

[1] J. Chay, H. Georgi, B. Grinstein, *Phys. Lett. B* 247 (1990) 399;  
 I.I.Y. Bigi, N.G. Uraltsev, A.I. Vainshtein, *Phys. Lett. B* 293 (1992) 430, hep-ph/9207214;  
 I.I.Y. Bigi, N.G. Uraltsev, A.I. Vainshtein, *Phys. Lett. B* 297 (1993) 477, Erratum;  
 I.I.Y. Bigi, M.A. Shifman, N.G. Uraltsev, A.I. Vainshtein, *Phys. Rev. Lett.* 71 (1993) 496, hep-ph/9304225;  
 A.V. Manohar, M.B. Wise, *Phys. Rev. D* 49 (1994) 1310, hep-ph/9308246.

<sup>1</sup> The structure of the differential equations indicates that  $\mathcal{I}_{1,2}(u, z)$  cannot be described by HPLs with simple arguments.

- [2] M. Beneke, G. Buchalla, M. Neubert, C.T. Sachrajda, Phys. Rev. Lett. 83 (1999) 1914, hep-ph/9905312; M. Beneke, G. Buchalla, M. Neubert, C.T. Sachrajda, Nucl. Phys. B 591 (2000) 313, hep-ph/0006124; M. Beneke, G. Buchalla, M. Neubert, C.T. Sachrajda, Nucl. Phys. B 606 (2001) 245, hep-ph/0104110.
- [3] C.W. Bauer, S. Fleming, D. Pirjol, I.W. Stewart, Phys. Rev. D 63 (2001) 114020, hep-ph/0011336; C.W. Bauer, D. Pirjol, I.W. Stewart, Phys. Rev. D 65 (2002) 054022, hep-ph/0109045; M. Beneke, A.P. Chapovsky, M. Diehl, T. Feldmann, Nucl. Phys. B 643 (2002) 431, hep-ph/0206152.
- [4] G.P. Korchemsky, G. Sterman, Phys. Lett. B 340 (1994) 96, hep-ph/9407344.
- [5] M. Neubert, Phys. Rev. D 49 (1994) 3392, hep-ph/9311325; I.I.Y. Bigi, M.A. Shifman, N.G. Uraltsev, A.I. Vainshtein, Int. J. Mod. Phys. A 9 (1994) 2467, hep-ph/9312359.
- [6] C.W. Bauer, A.V. Manohar, Phys. Rev. D 70 (2004) 034024, hep-ph/0312109; S.W. Bosch, B.O. Lange, M. Neubert, G. Paz, Nucl. Phys. B 699 (2004) 335, hep-ph/0402094.
- [7] T. Becher, M. Neubert, Phys. Lett. B 637 (2006) 251, hep-ph/0603140.
- [8] R. Bonciani, A. Ferroglia, arXiv: 0809.4687 [hep-ph].
- [9] G. Bell, Nucl. Phys. B 795 (2008) 1, arXiv: 0705.3127 [hep-ph]; G. Bell, PhD thesis, LMU München, 2006, arXiv: 0705.3133 [hep-ph]; G. Bell, in preparation.
- [10] F.V. Tkachov, Phys. Lett. B 100 (1981) 65; K.G. Chetyrkin, F.V. Tkachov, Nucl. Phys. B 192 (1981) 159.
- [11] S. Laporta, Int. J. Mod. Phys. A 15 (2000) 5087, hep-ph/0102033.
- [12] A.V. Kotikov, Phys. Lett. B 254 (1991) 158; E. Remiddi, Nuovo Cimento A 110 (1997) 1435, hep-th/9711188.
- [13] E. Remiddi, J.A.M. Vermaseren, Int. J. Mod. Phys. A 15 (2000) 725, hep-ph/9905237; D. Maitre, Comput. Phys. Commun. 174 (2006) 222, hep-ph/0507152.
- [14] V.A. Smirnov, Phys. Lett. B 460 (1999) 397, hep-ph/9905323; J.B. Tausk, Phys. Lett. B 469 (1999) 225, hep-ph/9909506; M. Czakon, Comput. Phys. Commun. 175 (2006) 559, hep-ph/0511200.
- [15] T. Binoth, G. Heinrich, Nucl. Phys. B 585 (2000) 741, hep-ph/0004013.
- [16] A.V. Smirnov, M.N. Tentyukov, arXiv: 0807.4129 [hep-ph].
- [17] N. Gray, D.J. Broadhurst, W. Grafe, K. Schilcher, Z. Phys. C 48 (1990) 673; D.J. Broadhurst, N. Gray, K. Schilcher, Z. Phys. C 52 (1991) 111.
- [18] T. Becher, M. Neubert, Phys. Lett. B 633 (2006) 739, hep-ph/0512208.
- [19] K.G. Chetyrkin, B.A. Kniehl, M. Steinhauser, Nucl. Phys. B 510 (1998) 61, hep-ph/9708255.
- [20] G.P. Korchemsky, A.V. Radyushkin, Nucl. Phys. B 283 (1987) 342; I.A. Korchemskaya, G.P. Korchemsky, Phys. Lett. B 287 (1992) 169.
- [21] M. Neubert, Eur. Phys. J. C 40 (2005) 165, hep-ph/0408179.
- [22] H.M. Asatrian, C. Greub, B.D. Pecjak, arXiv: 0810.0987 [hep-ph].
- [23] M. Beneke, T. Huber, X.Q. Li, arXiv: 0810.1230 [hep-ph].